

Simulating Wave Reflection Using Radiation Boundary

Mark J. Clyne and Thomas P. Mullarkey

Civil Engineering Department
National University of Ireland
Galway, Ireland
mark.clyne@nuigalway.ie



ABSTRACT

CLYNE, M.J. and MULLARKEY, T.P., 2008. Simulating wave reflection using radiation boundary. *Journal of Coastal Research*, 24(1A), 40–48. West Palm Beach (Florida), ISSN 0749-0208.

A finite element wave propagation model for linear periodic waves in a coastal sea region is developed. The model includes refraction, diffraction, and reflection of gravity waves on water over arbitrary bathymetry. The authors discuss the use of the computer model in simulating waves using a number of classical examples involving a circular pile, submerged shoal, and breakwater. The method of solution involves complex potential theory. The equation used by BERKHOFF (1976; *Mathematical Models for Simple Harmonic Linear Water Waves—Wave Diffraction and Refraction*. Delft: Delft Hydraulics Laboratory, Delft University of Technology, p. 111) and the authors within the domain is elliptic in type allowing wave trains to cross, thereby producing amphidromic points. An amphidromic point is the two-dimensional version of a node in a one-dimensional standing wave caused by imperfect reflection or wave train interference. Radiating and partially reflecting boundaries are modelled by the authors, using a parabolic equation developed in different ways by RADDER (1979; *On the parabolic equation method for water-wave propagation*, *Journal of Fluid Mechanics*, 95, 159–176) and BOOIJ (1981; *Gravity waves on water with non-uniform depth and current*. Delft: Delft Hydraulics Laboratory, Delft University of Technology, p. 127), allowing the passage of energy through a boundary over arbitrary bathymetry. RADDER (1979) and BOOIJ (1981) develop this equation in the domain as an alternative to the elliptic equation. BERKHOFF (1976) uses a downstream radiation boundary condition based on Hankel functions for the shoal problem, valid only in constant depth. The upstream boundary condition of BERKHOFF (1976) for the same shoal problem is derived using the wave ray method. The limitation of the wave ray method is that for general purposes the rays frequently cross, resulting in no solution. The method used by the authors has the advantage of simplicity in that the boundary conditions are very simple to implement but none of the physical features are lost.

ADDITIONAL INDEX WORDS: *Finite element, wave model, refraction, diffraction, reflection, amphidromic points.*

INTRODUCTION

In this paper the authors develop a wave propagation model capable of simulating refraction, diffraction, and total reflection using complex potential theory with an elliptic equation in the domain and a parabolic equation for the absorbing and radiating boundary conditions. Propagation of water waves is a phenomenon of great importance to coastal engineering practice. It is very difficult to develop a numerical model that describes all the physical processes involved in wave propagation; therefore, some simplifications must be made and only predominant processes are modelled. Fully three-dimensional solutions would be too complex to develop and are not practical to solve, since they are computationally expensive; hence, the dimension of the problem is reduced to two. BERKHOFF (1976) develops an elliptic-type mathematical equation, known as the mild-slope equation, to simulate diffraction, refraction, combined diffraction–refraction, and reflection of water waves around obstacles and over varying bathymetry. BOOIJ (1981) develops additional terms in order to include the effects of currents in the elliptic form of the mild-slope equation and then simplifies the model into a par-

abolic form, useful when modelling large domains because of its computational efficiency.

In this paper the authors develop an elliptic wave equation based on the mild-slope equation for use as the domain equation. Given the elliptic nature of the domain equation, energy is capable of travelling in all directions within the domain; therefore, an absorbing boundary condition is required. The authors develop such a boundary condition from the parabolic equations of RADDER (1979) and BOOIJ (1981). For certain model configurations wave reflections and backscattering of wave energy may occur; in this instance open boundaries require a radiation boundary condition. BERKHOFF (1976), as well as ISAACSON and QU (1989), uses Hankel functions to produce a radiation condition; however, Hankel functions are only valid in constant depth. THOMPSON, CHEN, and HADLEY (1996) and OLIVEIRA and ANASTASIOU (1998) develop a simple form of the radiation boundary condition that doesn't involve Hankel functions. XU *et al.* (1996) develops a parabolic radiation condition in polar coordinates with an elliptic domain equation, whereas the authors develop a radiation boundary condition from the parabolic equation of BOOIJ (1981) in Cartesian coordinates that is valid in arbitrary depth and can also include such physical features as energy dissipation and nonuniform currents. Comparisons are made between the results of the authors and those of BERKHOFF

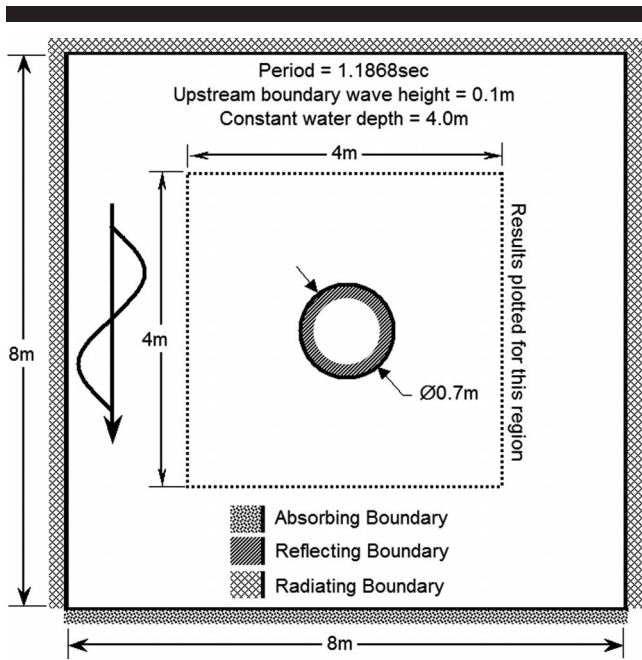


Figure 1. Layout of reflecting pile numerical model.

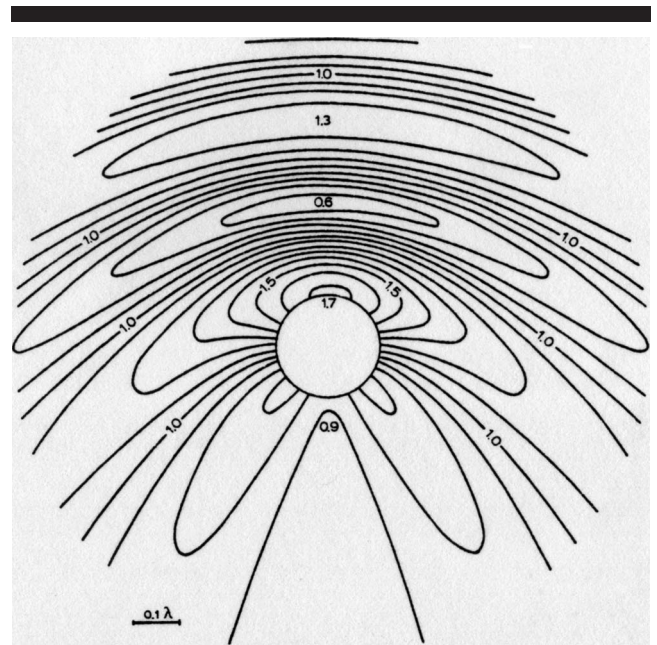


Figure 3. The solution of Berkhoff (1976) for normalised wave height (0.1 unit intervals).

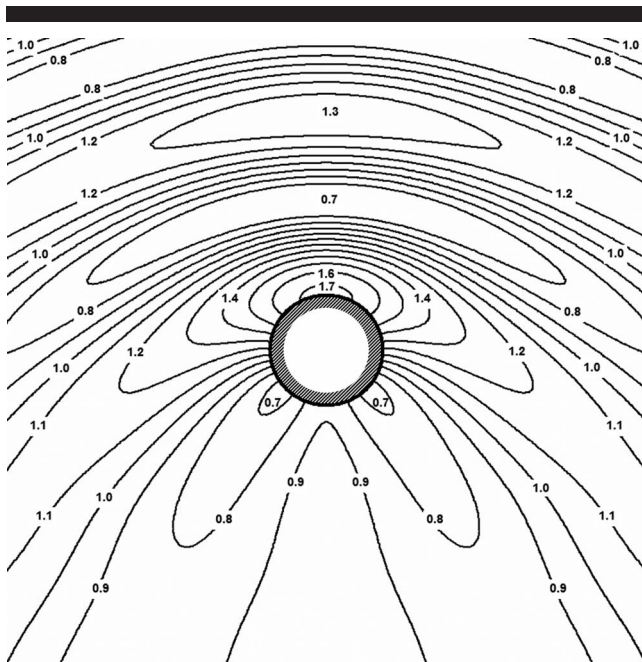


Figure 2. Authors' solution for normalised wave height (0.1 unit intervals).

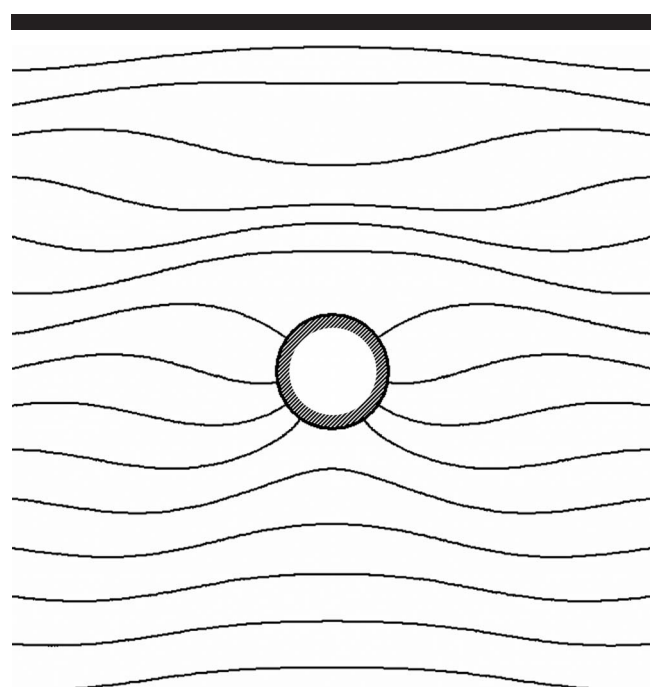


Figure 4. Authors' solution for wave phase ($\pi/4$ radian intervals).

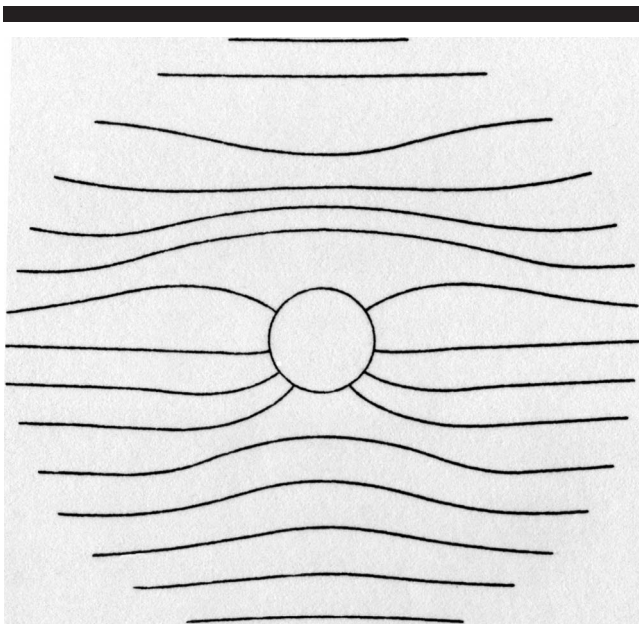


Figure 5. The solution of Berkhoff (1976) for wave phase ($\pi/4$ radian intervals).

(1976) for three classical problems. Harbour resonance is investigated using the analytical solution of MEI (1994), which is also solved numerically by BELLOTTI, BELTRAMI, and GIROLAMO (2003); finally, concluding remarks are made.

FUNDAMENTAL EQUATIONS

The mild-slope equation developed by BERKHOFF (1976) is applied here:

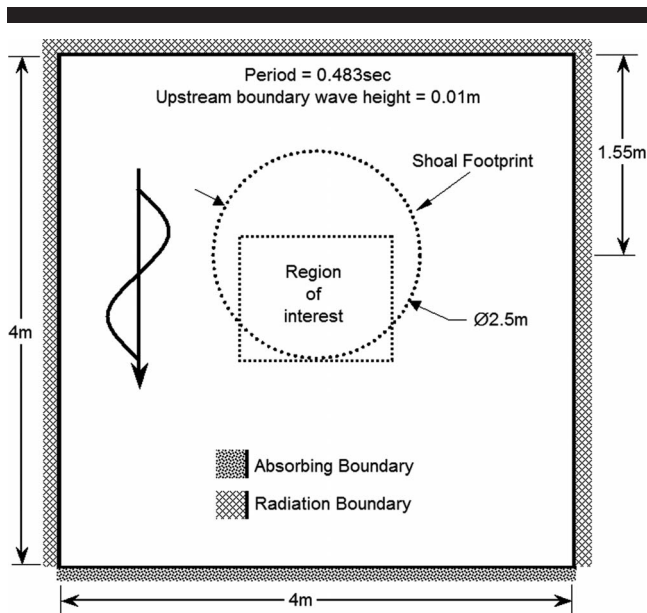


Figure 6. Layout of circular shoal numerical model.

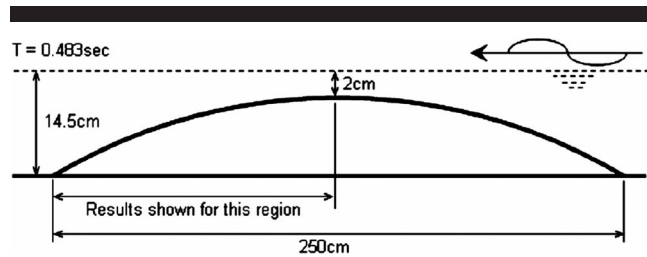


Figure 7. Parabolic profile of circular shoal.

$$\nabla(a\nabla\phi) + \kappa^2 a\phi = 0 \tag{1}$$

where $a = cc_g$ is the product of celerity and group velocity, κ is the local wave number, $\nabla = (\partial/\partial x)\mathbf{i} + (\partial/\partial y)\mathbf{j}$ is a two-dimensional differential operator, and ϕ is the two-dimensional complex velocity potential independent of time. Equation 1 is the result of the vertical integration of an original equation governing Φ , the three-dimensional potential including time, where a hyperbolic function is used to represent the vertical dimension. A periodic function is also included to eliminate the dependence of the potential on time t as shown in Equation 2:

$$\Phi(\mathbf{x}, z, t) = \frac{\cosh \kappa(z + d)}{\cosh \kappa d} \tilde{\phi}, \tag{2}$$

where $\tilde{\phi} = \text{Re}\{e^{-i\omega_0 t}\}\phi(\mathbf{x})$, z is the vertical dimension measured upward from the still water level, d is the local water depth, t is time, \mathbf{x} is the two-dimensional space of x and y , and ω_0 is frequency observed from a fixed point. Calculation of the wave number is carried out at every node in the domain by finding the root of the dispersion equation shown in Equation 3.

$$\omega_0^2 = g\kappa \tanh(\kappa d) \tag{3}$$

where g is the acceleration due to gravity.

The absorbing boundary condition, using the parabolic equation of BOOIJ (1981) in the absence of current, is substituted into the boundary integrals of the domain equation containing $\partial\phi_1/\partial n$ and $\partial\phi_2/\partial n$. The parabolic equation of BOOIJ (1981) contains two constants P_1 and P_2 . The constants are

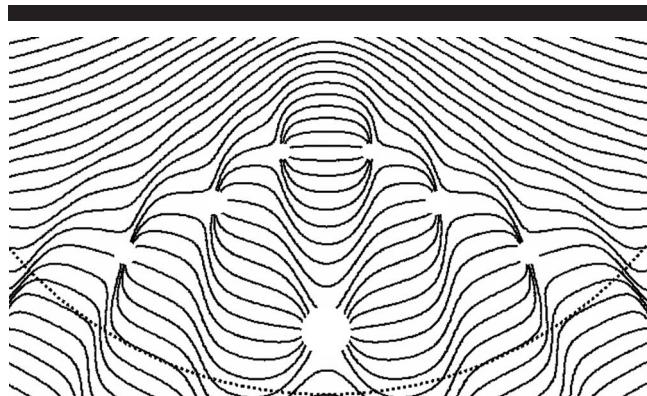


Figure 8. Authors' solution for wave phase ($\pi/4$ radian intervals).

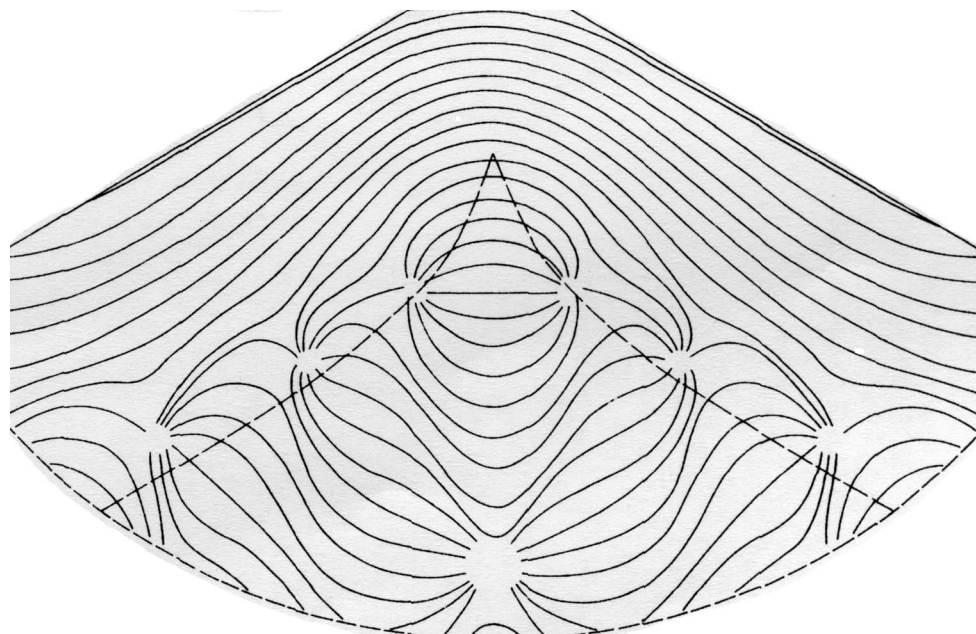


Figure 9. The solution of Berkhoff (1976) for wave phase ($\pi/4$ radian intervals).

related as follows: $P_2 = P_1 + 0.5$, resulting from a binomial expansion of wave number terms. P_1 and P_2 do not approximate Equation 1 if the difference between P_1 and P_2 is something other than 0.5, which was confirmed to the authors by BOOLJ (personal communication). The authors use $P_1 = 0.0$ and $P_2 = 0.5$, reducing the equation to the same one as that of RADDER (1979). RADDER (1979) uses a matrix splitting method to produce his parabolic equation, whereas BOOLJ (1981) uses the pseudo-operator method. The parabolic equation of RADDER (1979) and BOOLJ (1981) is as follows (terms containing P_1 are omitted since $P_1 = 0.0$),

$$\frac{\partial \phi}{\partial n} = \left[i\kappa - \frac{1}{2a\kappa} \frac{\partial(a\kappa)}{\partial n} + \frac{iP_2}{a\kappa} \frac{\partial}{\partial s} \left(a \frac{\partial}{\partial s} \right) \right] \phi = f(\phi) \quad (4)$$

where s is tangential to the boundary and perpendicular to n the outward normal and i is the imaginary operator where $i = \sqrt{-1}$. An extension of the absorbing boundary condition is the radiation boundary condition, which uses the parabolic absorbing equation to allow backscattered wave energy to pass through a boundary while containing the incident wave information. In order to develop the radiation condition, the full potential must be separated into its incident and scattered components shown in Equation 5, the scattered potential obeying Equation 4.

$$\begin{aligned} \phi &= \phi^I + \phi^S & \phi^S &= \phi - \phi^I \\ \frac{\partial \phi^S}{\partial n} &= f(\phi^S) & \frac{\partial}{\partial n}(\phi - \phi^I) &= f(\phi - \phi^I) \\ \frac{\partial \phi}{\partial n} &= f(\phi) - f(\phi^I) + \frac{\partial \phi^I}{\partial n} \end{aligned} \quad (5)$$

where $f(\phi)$ is the right-hand side of Equation 4, ϕ^S is the unknown scattered potential, and ϕ^I is the known incident potential developed from one-dimensional solutions along the required boundaries. After the solution is completed the complex potential $\phi = \phi_1 + i\phi_2$ is converted into the complex water surface elevation:

$$\eta = i \frac{\omega_0}{g} \phi, \quad (6)$$

where $\eta = \eta_1 + i\eta_2$.

The complex water surface elevation η in Equation 6 is combined with a periodic function to produce the real water surface for an arbitrary value of time t , as seen in Equation 7.

$$\tilde{\eta}(\mathbf{x}, t) = \text{Re}\{e^{-i\omega_0 t} \eta(\mathbf{x})\} = \eta_1 \cos \omega_0 t + \eta_2 \sin \omega_0 t. \quad (7)$$

RESULTS

The authors will verify their solutions below using three of the classical problems of BERKHOFF (1976): the circular reflecting pile, the semi-infinite breakwater, and the circular shoal. And the authors verify their simulation of harbour resonance by means of the analytical solution of MEI (1994).

Reflecting Pile

To simulate wave propagation around a perfectly reflecting cylinder of a circular cross section, a finite element model is generated using triangular elements as per the configuration in Figure 1. A wave of period 1.1868 seconds propagates from the top to the bottom of the domain over a constant water depth of 4.0 m, with an upstream boundary wave height of 0.1 m.

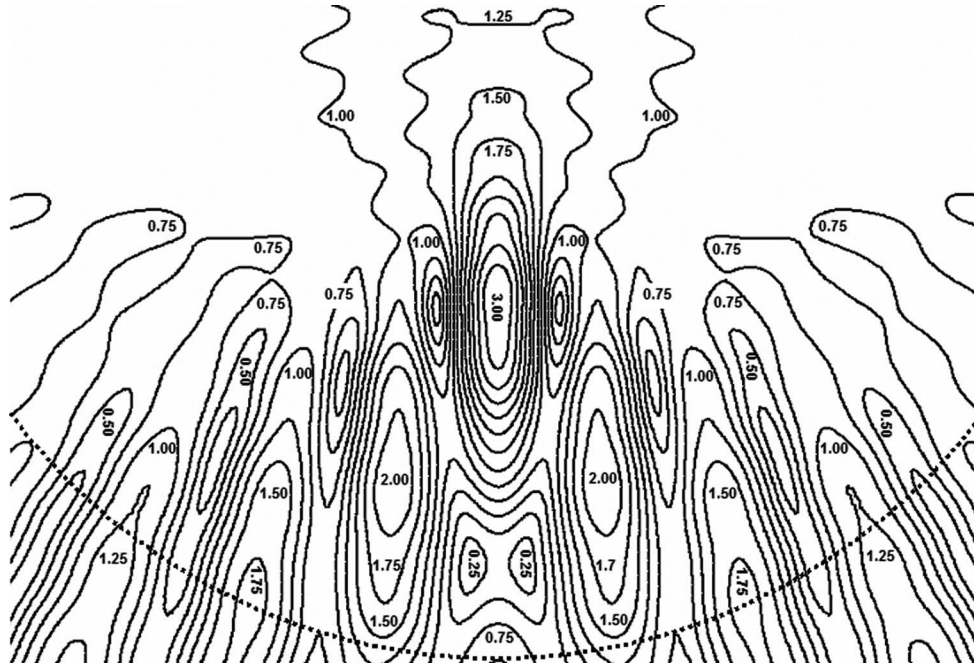


Figure 10. Authors' solution for normalised wave height (0.25 unit intervals).

Following the authors' numerical solution, a plot for normalised wave height, *i.e.*, height divided by incident height, is produced as seen in Figure 2, which illustrates the variation in wave height due to reflection and diffraction of wave energy.

Boundaries have been placed away from the area of interest to prevent them from adversely affecting the solution. Large wave heights occur upstream of the pile, where an antinode occurs at the perfectly reflecting boundary of the pile. Wave energy travels around the pile due to diffraction, the sheltering effect of the pile leads to low wave height on the downstream boundary of the pile. The authors' numerical solution in Figure 2 compares well with the analytical solution of BERKHOFF (1976) shown in Figure 3.

Figure 4 shows the pattern of wave crests, or phase lines, formed when waves propagate around a reflecting pile. Downstream of the pile a diffraction pattern is observed where the phase lines maintain an angle of 90° with the surface of the pile. Upstream of the pile the reflection field causes wavelengths to change because of the interaction of incident waves with scattered ones.

Very good agreement can be seen between the authors' numerical solution in Figure 4 and the analytical solution of BERKHOFF (1976) in Figure 5.

Circular Shoal

To demonstrate the behaviour of gravity waves propagating over a circular shoal, the numerical model shown in Figure 6 is developed. Boundaries have been placed away from the area of interest to prevent them from adversely affecting the solution.

Wave refraction, diffraction, and backscattering occur from the raised portion of the seabed whose parabolic profile is illustrated in Figure 7.

Phase lines form the pattern in Figure 8 over the shoal. Upstream of the shoal the phase lines are distinct and vary slowly as they refract over the reducing depths, in contrast to the complicated pattern of wave diffraction and interactions occurring downstream of the crest of the shoal, which causes the occurrence of amphidromic points where wave trains overlap.

Very good agreement is observed between the plots of the authors' numerical solution in Figure 8 and that of BERKHOFF (1976) in Figure 9. The location and number of amphidromic points or nodes compare very well also.

Wave energy focusing occurs just downstream of the crest of the shoal, with a magnitude of three times that of the incident wave energy illustrated by the maximum in Figure 10. It can be seen from comparison of Figure 8 with Figure 10 that at amphidromic points the wave height approaches zero.

Figure 11 shows that the solution of BERKHOFF (1976) for normalised wave height produces a larger maximum than that of the authors in Figure 10. This is due to differences in the boundary conditions used. BERKHOFF (1976) uses a constrained upstream boundary with incident wave data taken from a ray solution, while the authors use a radiation boundary condition upstream and on the two sides to allow the backscattering of wave energy out of the domain.

Semi-Infinite Breakwater

To investigate the behaviour of waves that propagate toward a reflecting semi-infinite breakwater, the numerical

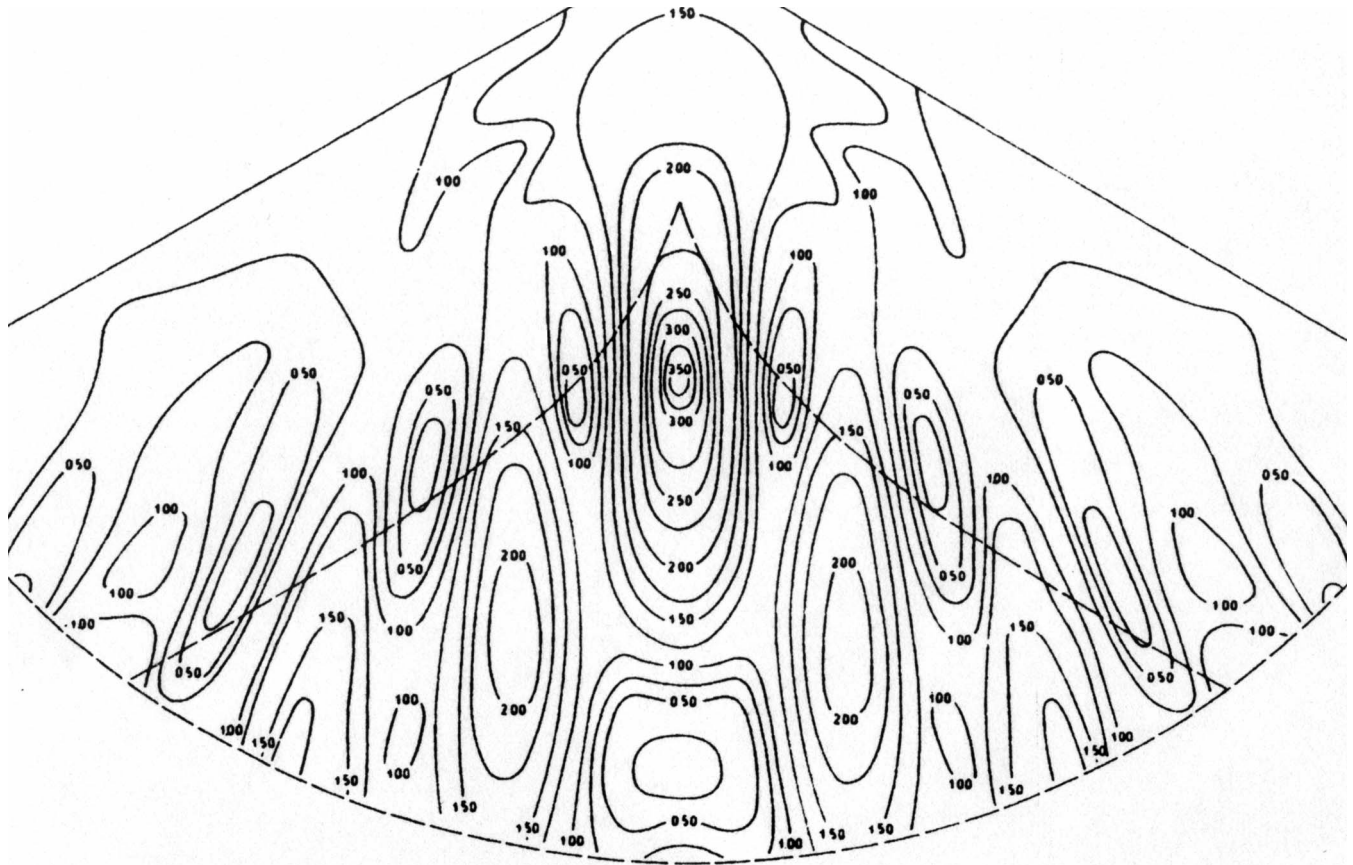


Figure 11. The solution of Berkhoff (1976) for normalised wave height (0.25 unit intervals).

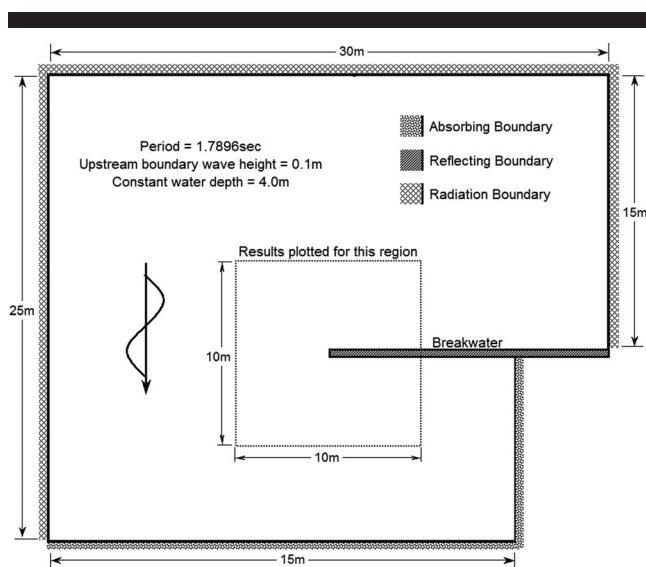


Figure 12. Layout of semi-infinite breakwater numerical model.

model in Figure 12 is used. Waves propagate in a direction normal to the breakwater and reflect from it, causing standing waves to occur while wave energy also diffracts around the tip of the breakwater and downstream of the breakwater. Boundaries have been placed away from the area of interest to prevent them from adversely affecting the solution. Waves incident on a reflecting breakwater exhibit the phase pattern shown in Figure 13, whereby the interaction of incident and reflected waves produces nodes or amphidromic points illustrated by the points of intersection of wave phase in Figure 13.

As waves diffract around the breakwater they maintain an angle of 90° with the downstream face of the breakwater. The complicated phase line pattern upstream of the breakwater is illustrated by the use of a small contour interval of 2.5° compared with the 20° intervals elsewhere.

The authors' numerical solution in Figure 13 is similar to the analytical solution of BERKHOFF (1976) in Figure 14. The authors' plot of normalised wave height in Figure 15 shows that there is a significant sheltering effect downstream of the breakwater as the wave height reduces to less than 25% of the incident value. Upstream of the breakwater wave heights vary rapidly from maximums to minimums. Positions where wave heights approach zero coincide with locations of phase

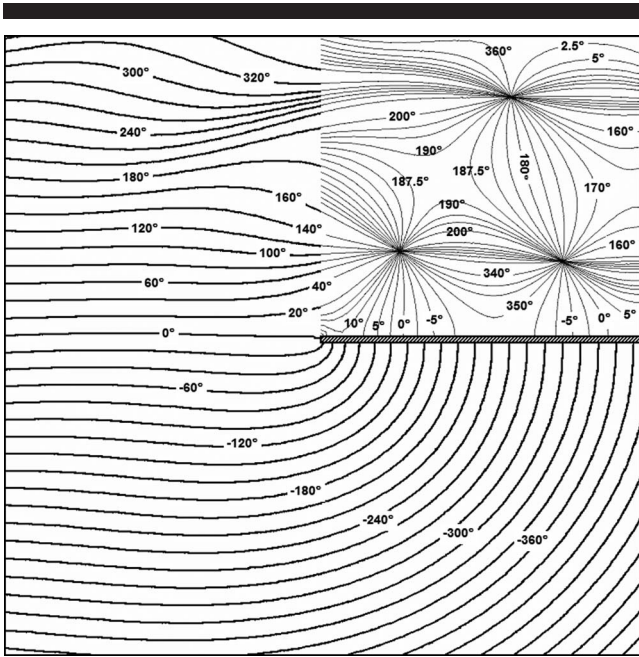


Figure 13. Authors' solution for wave phase (2.5 and 20 degree intervals).

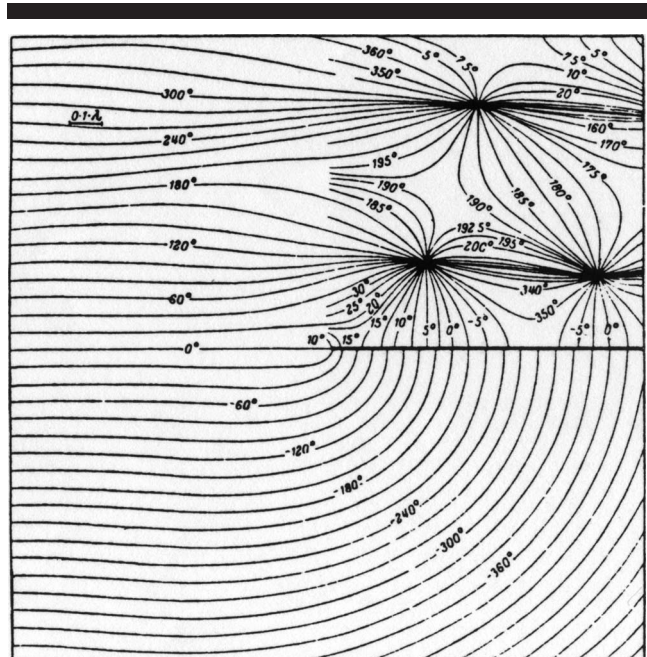


Figure 14. The solution of Berkhoff (1976) for wave phase (2.5 and 20 degree intervals).

line intersections known as amphidromic points, this is evident when comparing Figure 13 with Figure 15.

The analytical solution of BERKHOFF (1976) in Figure 16 is similar to the authors' numerical solution in Figure 15.

Harbour Resonance

A narrow bay of finite length shown in Figure 17 illustrates many common features of harbour resonance. The nodal density of the mesh in Figure 17 is such that for the smallest period there are approximately 30 nodes per wavelength. In order to model the waves for this type of harbour configuration the solution is separated into two parts. First an analytical solution of the standing wave against the straight coastline is calculated. Second waves are simulated with the harbour present, which causes scattered waves to propagate out from the harbour mouth. Open boundaries are subject to the radiation boundary condition, which contains incident wave data in the form of the analytical standing wave calculated prior to solution.

Separating the solution into two parts allows the two sets of scattered waves, namely, the reflected waves from an infinitely long cliff and the scattered waves from the harbour, to be modelled independently. Modelling the problem as one set of scattered waves causes the reflected wave from the straight boundary to be distorted as a result of the superposition of this wave with the scattered wave from the mouth of the harbour. The analytical solution of MEI (1994), Equa-

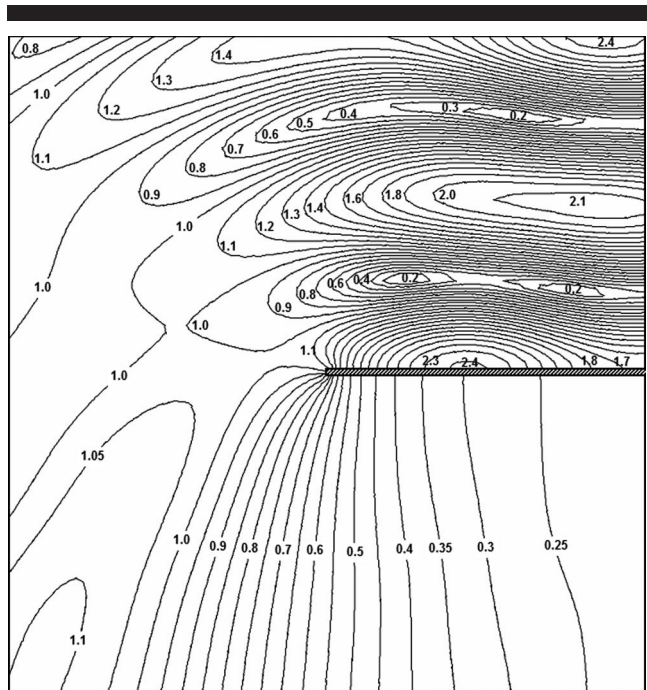


Figure 15. Authors' solution for normalised wave height (0.1 and 0.05 unit intervals).

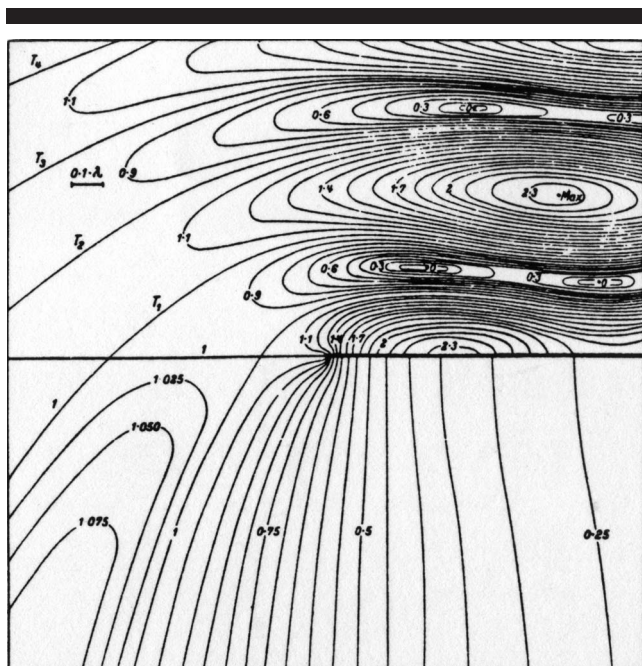


Figure 16. The solution of Berkhoff (1976) for normalised wave height (0.1 and 0.05 unit intervals).

tion 8 for the amplification factor due to harbour resonance in this type of bay, is illustrated in Figure 18.

$$C_a = \frac{1}{\cos \kappa L + (2\kappa a/\pi)\sin \kappa L \ln(2\gamma\kappa a/\pi e) - i\kappa a \sin \kappa L} \quad (8)$$

where L is the length of the harbour, a is half the width of the harbour, e is the base of the natural logarithm ($e = 2.71828...$), and γ is Euler's constant; however, in this instance MEI (1994) redefines Euler's constant to be $\ln \gamma = 0.5772157$, for tidier notation. As part of the derivation of Equation 8 by MEI (1994), an inner approximation using the ABRAMOWITZ and STEGUN (1972) expansion of the far-field solution for a standing and radiating wave in the vicinity of the harbour entrance reduces the term containing a $H_0^{(1)}$ Hankel function in the far-field solution to two terms in the approximation, one of which contains γ . The ABRAMOWITZ and STEGUN (1972) expansion is based on an ascending series for small values of the general complex independent variable; in this case MEI (1994) uses the real form of the independent variable. The authors calculate the numerical amplification factor using Equation 9, where $H_{incident}$ is the incident wave height and $H_{recorded}$ is the recorded height at the end of the channel at the centre of the back wall.

$$C_a = \frac{1}{2} \frac{H_{recorded}}{H_{incident}} \quad (9)$$

Derivation of the analytical solution of MEI (1994) consists of this technique of separating the scattered wave into its two components, the reflected wave from the straight coastline plus the scattered wave from the harbour. Good agreement is found when comparing the authors' numerical solution

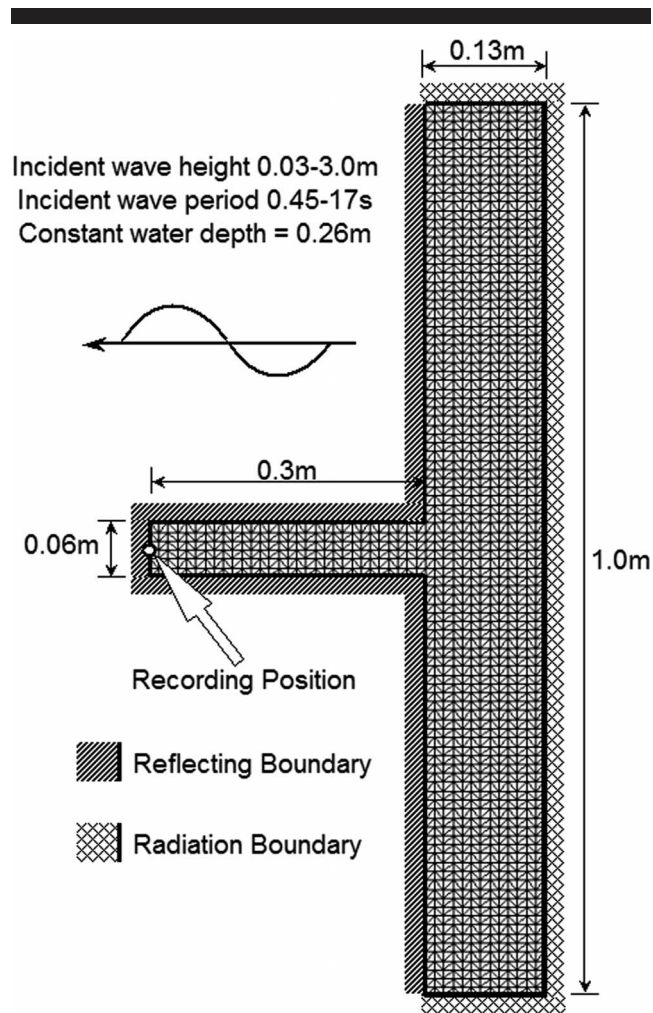


Figure 17. Layout of harbour resonance numerical model.

with the analytical solution of MEI (1994) in Figure 18. In Figure 18 the harbour length is 0.3 m. Some relevant values extracted from Figure 18 are as follows: at the larger peak the wavelength is just less than five times the harbour length, and at the smaller peak it is just less than 1.5 times the harbour length. Numerical simulation generates an amplification factor of somewhat greater magnitude than the analytical solution at the larger peak; this may be due in part to the size of the domain, since at the larger peak the length of the wave is much greater than the harbour length for this resonance event. The amplification factor at the second peak is in better agreement.

CONCLUSIONS

The examples in the results section are chosen to test the performance of the radiation boundary condition by subjecting it to various forms of radiated and scattered wave energy from different shaped reflecting obstacles, boundaries, and seabed features. In all the examples presented the results have been very favourable for the authors' model when com-

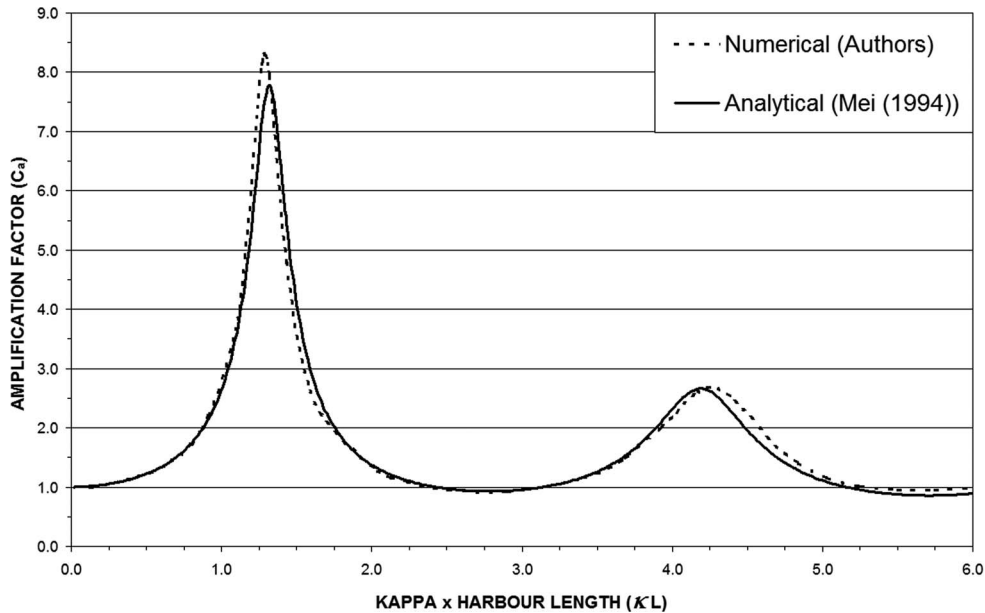


Figure 18. Amplification factors for a long and narrow bay.

pared to the literature, indicating that the radiation boundary condition is performing very well. Further testing the scope and flexibility of the model is the example of harbour resonance, since this problem places significant demand on the radiation boundary over a wide spectrum of wave periods to produce the amplification factor plot for the chosen harbour. In general the radiation boundary condition acts as a dampening mechanism, in this case allowing excess energy to escape from the harbour. The parabolic radiation and absorbing boundary condition combined with the elliptic-type domain equation delivers results of a high quality for a wide range of problems with a wide spectrum of wave frequencies.

LITERATURE CITED

- ABRAMOWITZ, M. and STEGUN, I.A., 1972. *Handbook of Mathematical Functions*. New York: Dover.
- BELLOTTI, G.; BELTRAMI, G.M., and GIROLAMO, P.D., 2003. Internal generation of waves in 2D fully elliptic mild-slope equation FEM models. *Coastal Engineering*, 49, 71–81.
- BERKHOFF, J.C.W., 1976. *Mathematical Models for Simple Harmonic Linear Water Waves—Wave Diffraction and Refraction*. Delft: Delft Hydraulics Laboratory, Delft University of Technology, p. 111.
- BOOLJ, N. 1981. *Gravity Waves on Water with Non-uniform Depth and Current*. Delft: Delft Hydraulics Laboratory, Delft University of Technology, p. 127.
- ISAACSON, M., and QU, S. 1989. Waves in a harbour with partially reflecting boundaries. *Coastal Engineering*, 14, 193–214.
- MEI, C.C., 1994. *The Applied Dynamics of Ocean Surface Waves*. Singapore: World Scientific.
- OLIVEIRA, F.S.B.S. and ANASTASIOU, K., 1998. An efficient computational model for water wave propagation in coastal regions. *Applied Ocean Research*, 20, 263–271.
- RADDER A.C., 1979. On the parabolic equation method for water-wave propagation. *Journal of Fluid Mechanics*, 95, 159–176.
- THOMPSON, E.F.; CHEN, H.S., and HADLEY, L.L., 1996. Validation of numerical model for wind waves and swell in harbors. *Journal of Waterway, Port, Coastal, and Ocean Engineering*, 122(5), 245–257.
- XU, B.; PANCHANG, V., and DEMIRBILEK, Z., 1996. Exterior reflections in elliptic harbour wave models. *Journal of Waterway, Port, Coastal, and Ocean Engineering*, 122(3), 118–126.